Spectroscopic Investigation on the Interaction of NCA0424, a Potent Antitumor Indoloquinoxaline Derivative, with DNA

Toshimasa ISHIDA,*[,a] Yoshitetsu MIHARA,[a] Yumiko HAMA,[a] Akemi HANATANI,[a] Mariko TARUI,[a] Mitsunobu DOI,[a] Shiro NAKAIKE,[b] and Kunihiro KITAMURA[b]

Department of Physical Chemistry, Osaka University of Pharmaceutical Sciences,[a] 4–20–1 Nasahara, Takatsuki, Osaka 569–1094, Japan and Research Center of Taisho Pharmaceutical Co., Ltd.,[b] 1–403 Yoshino-cho, Ohmiya, Saitama 330, Japan. Received November 10, 1997; accepted January 9, 1998

NCA0424 (1), an indoloquinoxaline derivative, has a potent antitumor activity against *in vitro* and *in vivo* tumor models. To elucidate its structure–activity relationship, the interactions with various B-form DNAs were investigated by thermal denaturation, viscosity and circular dichroism (CD) measurements. The thermal stability of the DNA duplex was increased by the interaction with 1, and preferable binding for alternative purine-pyrimidine base sequence was suggested. Comparative viscometric measurements with ethidium bromide (an intercalator) and distamycin (a minor groove binder) suggested that 1 is an intercalator. The interaction of DNA with 1 revealed a new CD band at 340—390 nm. Taking advantage of this induced CD band, the equilibrium binding constants were determined for various DNAs, and the binding preference of 1 for the alternative purine-pyrimidine base sequence, especially for the case of guanine as purine base, was indicated. The appearance of the induced CD band implies the importance of 1 side chain for the effective and/or stable intercalation of the aromatic ring into the DNA base pair.

Key words indoloquinoxaline; DNA; intercalation; thermal stability; viscosity; induced CD

2-Methyl-2-[(6-methyl-6*H*-indolo[2,3-*b*]quinoxaline-4-yl)methylamino]-1,3-propanediol [NCA0424 (**1**), Fig. 1] is worthy of remark as a novel antitumor agent against *in vitro* and *in vivo* tumor models.[1)] Generally it has been accepted that the pharmacological properties of numerous antiviral and antitumor agents result from the multiple phenomena of the interaction with DNA, inhibitory effects directed towards topoisomerases, and many other processes such as DNA replicative or repair enzymes. The potent antitumor activity of **1** also may belong to this category, because it exhibits the inhibitory activity against topoisomerase II.[1)] In contrast with the physiological and pharmacological characterization of **1**, however, the nature of the mode of interaction with DNA, which would be essentially associated with its antitumor activity, is far from being fully understood.

Recently, we reported the intercalation mode[2)] of NC-182 (Fig. 1) for DNA, the antitumor activity of which is believed to be due to the inhibition of DNA synthesis and DNA topoisomerase activity.[3)] As a series of spectroscopic analyses on the DNA–antitumor drug interactions, we report here the DNA-interaction mode of **1**, based on the UV, viscosity and circular dichroism (CD) measurements and the comparison with the spectral data of NC-182, ethidium bromide (EtBr, a typical intercalator) and distamycin (Dist., a typical minor-groove binder specific for A-T sequence); **1** is superior to NC-182 in its solubility in water. Information on how **1** recognizes a particular DNA base sequence and/or how the DNA-binding mode is changed by the difference between the

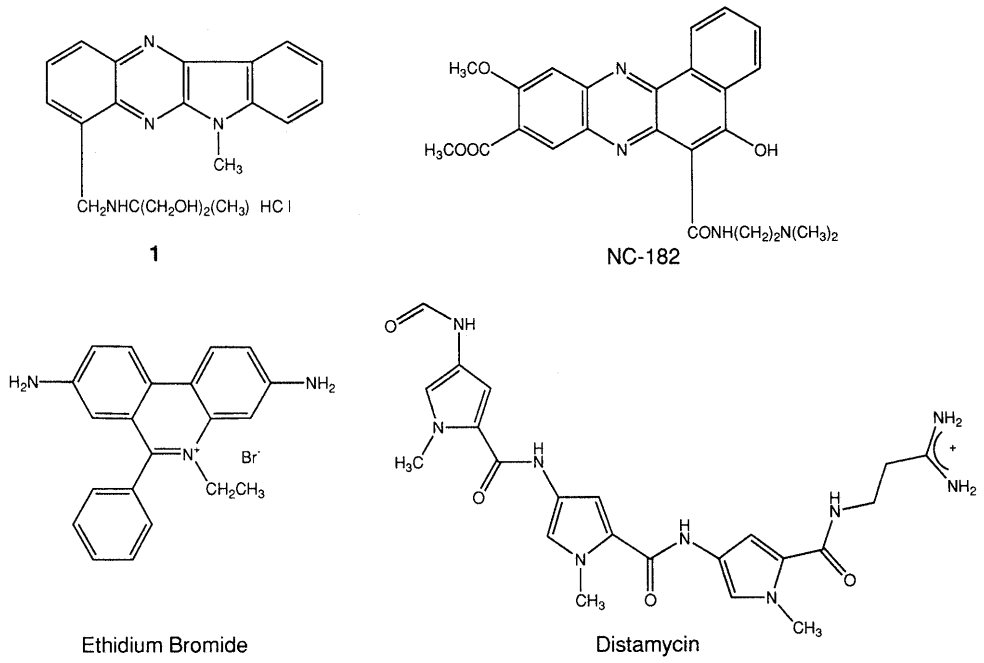

Fig. 1. Chemical Structures of **1**, NC-182, Ethidium Bromide (EtBr) and Distamycin (Dist.)

* To whom correspondence should be addressed.

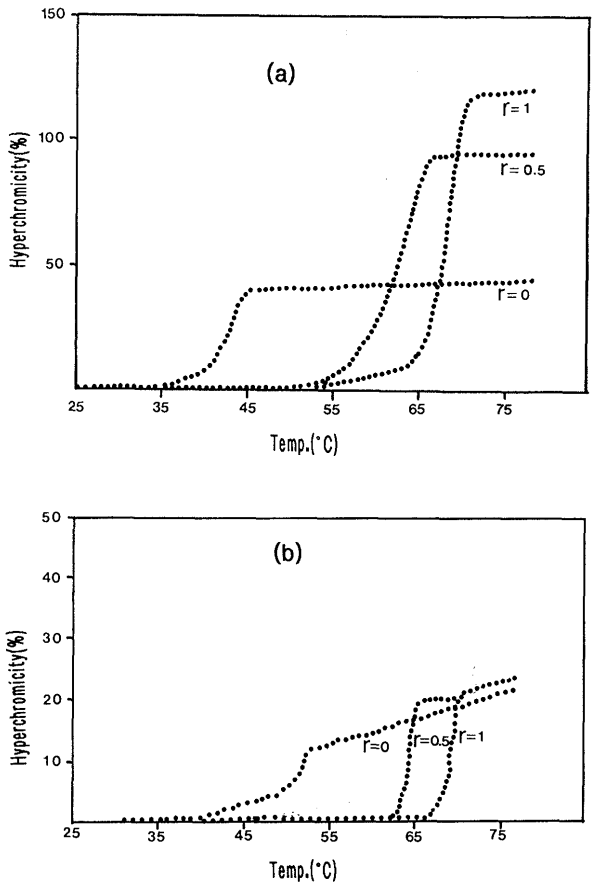

Fig. 2. UV Melting Curves of Poly(dA–dT) (a) and Poly(dA)·poly(dT) (b) Duplexes as a Function of r

chemical structures of **1** and NC-182 is essential as the first step for understanding the molecular basis of its antitumor activity and is of special importance for further development of clinically usable drugs.

Thermal Stabilization of DNA Duplex by 1 Figure 2 exemplifies the UV melting curves (optical density variations at 260 nm as a function of temperature) of poly(dA–dT) (a) and poly(dA)·poly(dT) (b) duplexes as a function of r. The changes of melting temperatures (T_m) for respective DNA species are given in Table 1. The T_m of poly(dA–dT) increased with the concentration of **1** in the range of $0<r<1$, and was almost saturated at $r=1$. There is a noteworthy difference between the melting profiles of poly(dA–dT) and poly(dA)·poly(dT) duplexes. The melting curve of poly(dA)·poly(dT) shows a transition profile with a broad and gentle slope in the range of $0<r<0.5$, and it becomes a steep profile at $r>0.5$. The former phenomenon could be interpreted as different conformations between the drug-bound and -unbound DNAs, which reflects the nonspecific or multiple DNA binding mode of the drug, as has been frequently observed in the T_m experiment of DNA.[4] In contrast, the steep profile of poly(dA–dT) duplex during $0<r<1$ could reflect the stoichiometric binding without multiple conformation. The result suggests the binding preference of **1** for alternative purine-pyrimidine base sequence.

To estimate the participation of guanine base in the DNA–**1** interaction, the thermal profiles of poly(dA–dG)·poly(dC–dT) and poly(dA–dC)·poly(dG–dT) duplexes were measured. While no remarkable change of ΔT_m was observed for poly(dA–dG)·poly(dC–dT) duplex (indicating no specific interaction), the steep ΔT_m profile of poly(dA–dC)·poly(dG–dT) duplex shifted to the high-temperature side in proportion to r and was almost saturated at $r>0.2$. Since the poly(dA–dC)·poly(dG–dT) duplex structure itself ($T_m=68.3$ °C) is thermally more rigid than the poly(dA–dT) structure ($T_m=42.5$ °C), the saturation of the former DNA at much lower r value than that of the latter one may imply the smooth binding of **1** to the guanine-pyrimidine base sequence without any notable conformational change of DNA, as compared with the binding to the adenine-pyrimidine sequence.

Table 1. Melting Temperatures (T_m) of Poly(dA–dT), Poly(dA)·poly(dT), Poly(dA–dC)·poly(dG–dT) and Poly(dA–dG)·poly(dC–dT) as a Function of r

r	Poly(dA–dT)	ΔT_m	Poly(dA)·poly(dT)	ΔT_m
0	42.5 °C		50.2 °C	
0.2	54.6	12.1	57.9	7.7
0.5	62.4	19.9	64.0	13.8
1.0	68.5	26.0	68.7	18.5
1.5	69.8	27.3	70.3	20.1
r	Poly(dA–dC)·poly(dG–dT)	ΔT_m	Poly(dA–dG)·poly(dC–dT)	ΔT_m
0	68.3 °C		75.4 °C	
0.02	70.2	1.9	76.0	0.6
0.05	71.5	3.2	76.4	1.0
0.1	75.1	6.8	76.9	1.5
0.15	76.2	7.9	77.3	1.9

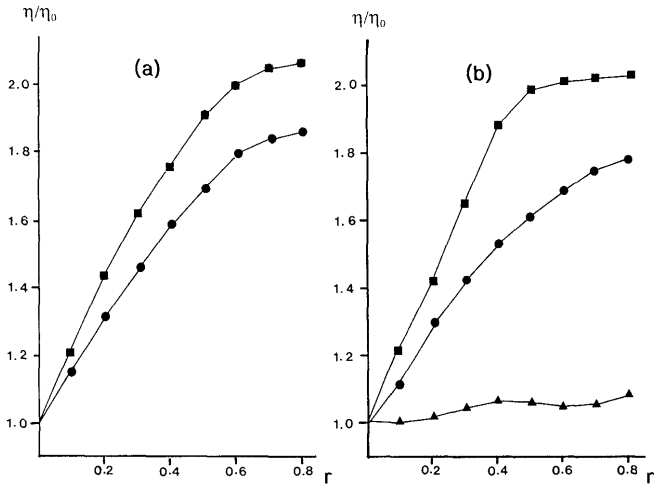

Fig. 3. Viscometric Titrations of B-Form Poly(dA–dT) (a) and Poly(dG–dC) (b) with **1** (—●—), EtBr (—■—) or Dist (—▲—)

Viscometric Studies The viscosity of DNA was measured in the presence of **1**, NC-182, EtBr or Dist to determine the interaction mode of **1** with DNA. The viscometric titrations of these drugs for poly(dG–dC) and poly(dA–dT) are shown in Fig. 3. The DNA viscosities were significantly increased by EtBr, but not by Dist. The increase by EtBr is primarily due to the lengthening of DNA structure by the intercalation of the drug.[5] Generally, it is known that the increment of the relative viscosity (η/η_0) by the binding of the drug is most

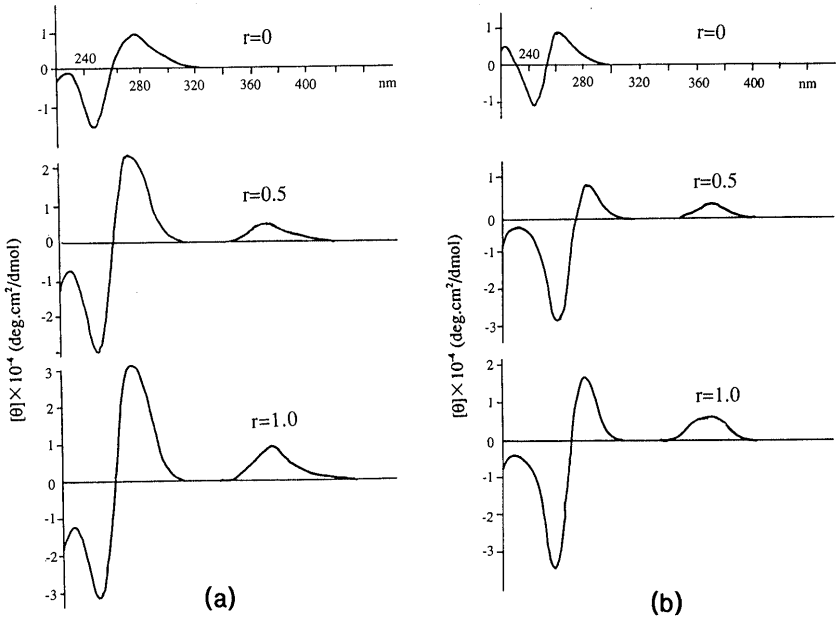

Fig. 4. CD Spectra for B-Form Poly(dG–dC) (a) and Poly(dA–dT) (b) as a Function of r
The concentration of DNA is 10 μM.

significant for B-form DNA, where the value is within the range of 1.9 ± 0.3 at the saturated state for the typical intercalator.[6] As judged from the η/η_0 profiles of EtBr and Dist measured as a function of r, the binding of **1** is suggested to be intercalative for both the poly(dA–dT) and poly(dG–dC) duplexes. Nearly the same viscometric result has been reported for NC-182[2] and Trp-P[7] (a potent mutacarcinogen isolated from tryptophan pyrolysate).

CD Studies CD spectra were measured to obtain the association constants and structural characteristics between **1** and various B-form DNAs [poly(dG–dC), poly(dA–dT), calf thymus (CT) DNA, poly(dA)·poly(dT), and poly(dG)·poly(dC)]; no CD band was observed in **1** alone.

1) 220—310 nm Region: The CD spectral changes for poly(dG–dC) (a) and poly(dA–dT) (b) are shown in Fig. 4. Similar to other DNA species, these CD spectra showed common changes in proportion to the increase of **1**, *i.e.*, i) the enlargement of the concomitant positive (*ca.* 270 nm) and negative (*ca.* 250 nm) ellipticities, which is typical of conservative B-form DNA, is **1**-dependent in the range of $0<r<1$, and ii) no notable CD change is observed at $r>ca.$ 1.0. In the former phase, **1** is thought to render the B-form DNA structures rigid, because the strength of CD ellipticity is dependent on the extent of stacking among DNA bases,[8] in addition to the contribution of the relative geometry of the bases (distance, twist, tilt, and so on); similar enlargement of B-form DNA has been observed for NC-182,[2] Trp-P-1[7] and EtBr.[9] Generally, such a spectral change could be interpreted in terms of intercalation-type binding, which leads to stiffening of DNA duplex structure as a result of DNA lengthening.[8] The saturation of the CD change at $r=ca.$ 1.0 indicates the 1 : 1 stoichiometry of **1** with respect to DNA base pair. Concerning this point, there is a notable difference from NC-182; the drastic decrease of the positive band at *ca.* 280 nm is caused by the addition of NC-182 at $r>1.0$, probably due to the transformation of the B-form DNA to a non-B-form structure.[2] Obviously, this has resulted from the different structural function between the side chains of **1** and NC-182 for the interaction with DNA, although the binding modes would both be intercalative.

2) 340—400 nm Region: Characteristically, a new CD band appeared at the 340—400 nm region ($\lambda_{max}=ca.$ 370 nm) with the addition of **1** (see Fig. 4), while such a band has not been observed for other drugs in Fig. 1. Since **1** itself has no CD band around this region, this induced CD (ICD) is clearly indicative of the complex formation with DNA. Since the CD band consists of the anisotropic absorption of plane polarized light and thus is revealed by the asymmetric environment of the sample, the ICD implies the formation of a new asymmetric (complex) structure by the binding of **1**.

The intensities of ICDs were proportionally increased in the range of $0<r<1$, where no changes in the shapes of ICD bands were observed for all investigated DNAs. The ICD values at λ_{max} within $r<1.0$ were therefore used in determining the equilibrium binding constant, K. The plots of $\Delta C_i/\Delta\rho_i$ *versus* $\Delta(C_i/\rho_i)/\Delta\rho_i$ for poly(dG–dC) and poly(dA–dT) are exemplified in Fig. 5. The straight line graphs confirm the uniformity of the binding mode of **1** against the DNAs. The K values, obtained from the least-squares analyses, are given in Table 2. The result suggests that **1** has a binding preference for the G-C or guanine-pyrimidine base sequence with the interaction site size being 2.2—2.6 base pairs. The result agrees well with the experiment on thermal stability.

NC-182 and EtBr, though these are typical intercalators, do not induce CD bands for DNAs. Thus, the formation of ICD could be noted as a characteristic feature of **1**. It is noteworthy that such a behavior results from the close interplay between the aromatic ring and side chain structure of **1** for the effective interaction with DNA; the side chain especially would play an important role in the formation of ICD, because the aromatic ring itself does

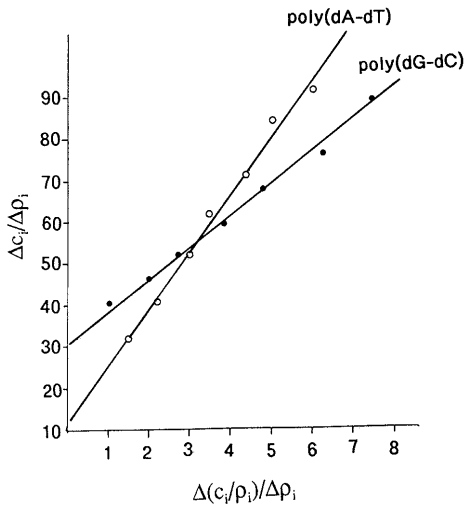

Fig. 5. Plots of $\Delta C_i/\Delta\rho_i$ *versus* $\Delta(C_i/\rho_i)/\Delta\rho_i$ for Poly(dG–dC) and Poly(dA–dT) with **1**

Table 2. Binding Constants for the Interaction of **1** with DNAs, Obtained from ICDs

DNA	$n^{a)}$	$K\times10^{-7}$ $(M^{-1})^{b)}$
Poly(dG–dC)	2.2	8.99
Poly(dA–dC)·poly(dG–dT)	2.6	8.69
Poly(dA–dT)	1.3	7.54
Poly(dA–dG)·poly(dC–dT)	1.5	6.97
Poly(dA)·poly(dT)	1.5	4.61
CT DNA	0.7	3.85

a) The value corresponds to the intercalation site size (in base pair units). *b*) The experimental errors are all within 10% of the given values.

not induce such a remarkable ICD band.

The potent antitumor activity of **1** toward various leukemias, fibrosarcomas and melanomas has been reported. The present study indicated the stoichiometric intercalation of **1** into the DNA base pair, especially into the base pair of guanine–pyrimidine sequence, and suggests that the antitumor activity of **1** *in vivo* is strongly due to such a specific binding with DNA at the concentration level of the living cell, in addition to the inhibitory activity against topoisomerase II.

Experimental

Materials Poly(dA–dT), poly(dG–dC), poly(dG–dT)·poly(dA–dC), poly(dA–dG)·poly(dC–dT), poly(dA)·poly(dT) and CT DNA were purchased from P-L Biochemicals and used without further purification. **1** (hydrochloride salt) and NC-182 were provided by Taisho Pharmaceutical Co., Ltd. All other chemicals used were of analytical grade, and the sample solutions were prepared with doubly distilled and deionized water.

Sample Preparation The solution of B-form DNA was adjusted with 10 mM sodium cacodylate buffer (pH 7.0, 25 °C). The measurements were carried out five times and each spectrum reported is an average of the five. DNA concentrations were determined using the standard molar extinction values ($M^{-1}cm^{-1}$) reported in the appended documents from P-L Biochemicals or in the literature[10] and were expressed in terms of moles of phosphate per liter. The molar extinction coefficients per base of the oligomers were calculated according to the method of Cantor *et al.*[11] The molar extinction coefficient of **1** was determined to be $\varepsilon_{418}=3536\,M^{-1}cm^{-1}$ using the gravimetrically prepared solution of 10 mM sodium cacodylate buffer, and was used for the determination of concentration. Measurements covering a comprehensive range of r were performed at a constant DNA concentration, where r is defined as the molar ratio of drug to DNA base pair.

Absorption Measurements UV melting curves of DNA samples were measured on a Jasco UVIDEC-610 spectrometer using 5-mm path-length cells, where the DNA concentration was adjusted to 10 μM (base pair), and drug concentration was varied as a function of r. The temperature was controlled by a circulating water bath. The optical density at 260 nm was monitored as a function of temperature, where the heating rate of sample solution was set to 0.5 °C/min. Under this condition, it was not possible to measure the melting point of poly(dG–dC), because the T_m was too high to be measured by this method.

Viscometric Measurements Viscometric measurements were conducted using a Cannon–Manning semimicrodilution viscometer (No. 75). The DNA concentration of 200 μM was prepared in 10 mM sodium cacodylate buffer. The temperature was set at 35 °C. A sample solution of 330 μl was placed in a viscometer, and the titration was conducted as a function of r.

CD Measurements CD spectra were recorded on a Jasco J-20C spectropolarimeter with a DP-500N data processor using 5-mm path-length cells. Sample temperature in the cuvette was regulated by a circulating water bath and was kept at 25 °C. A 10 μM concentration (base pair) of DNA solution was used for the measurements and the CD spectral change was monitored as a function of r. The molar ellipticity $[\theta]$ $(deg\cdot cm^2\cdot dmol^{-1})$ was calculated from the equation, $[\theta]=100\times\theta_{obsd.}/lC_p$, where $\theta_{obsd.}$ is the measured ellipticity in degrees, C_p is the DNA concentration in terms of phosphate, and l is the path-length in centimeters. The measurement of each CD spectrum was repeated 5—6 times and checked for possible base line shift.

Provided that one binding mode (or constant proportions of a number of modes) was present over a range of drug concentration, the equilibrium binding constant (K) of **1**–DNA complex could be evaluated from the ICD according to the following equation[12]:

$$\frac{\delta C_i}{\delta\rho_i}=\left(\frac{d}{\alpha}\right)\left[\frac{\delta(C_i/\rho_i)}{\delta\rho_i}\right]+\alpha,$$

$$K=\frac{\alpha\rho}{(d-\alpha\rho)(C_{tot}-\alpha\rho)},$$

where δC_i is the difference between the ith and kth concentrations of drug, $\delta\rho_i$ is the difference between the ith and kth ICDs, $\delta(C_i/\rho_i)$ is the difference between the C_i/ρ_i and C_k/ρ_k values, d is the concentration of binding sites on the DNA ($d=C_M/n$, where C_M=the concentration of DNA, n=the effective site size), $\alpha\rho$ ($=C_b$) is the bound concentration of drug, and C_{tot} is the total concentration of drug. For a constant DNA concentration, a plot of $\Delta C_i/\Delta\rho_i$ *versus* $\Delta(C_i/\rho_i)/\Delta\rho_i$ gives a straight line with slope d/α and intercept α. The n and K values are obtained from the above equation by the least-squares linear regression analyses.

Acknowledgments This work was supported by a Grant-in-Aid for Scientific Research on Priority Areas (No.06240104) from the Ministry of Education, Science, Sports and Culture, Japan.

References

1) Samata K., Yamagishi T., Ichihara T., Okado N., Ikeda T., Nakaike S., Nagate T. Abstracts of Papers, 56th Annual Meeting of Japan Cancer Association, Kyoto, September 1997, p. 620.
2) Tarui M., Doi M., Ishida T., Nakaike S., Kitamura K., *Biochem. J.*, **304**, 271—279 (1994).
3) *a*) Nakaike S., Yamagishi T., Nanaumi K., Otomo S., Tsukagoshi S., *Jpn. J. Cancer Res.*, **83**, 402—409 (1992); *b*) Tsuruo T., Naito M., Takamori R., Tsukahara S., Yamabe-Mitsuhashi J., Yamazaki A., Oh-hara T., Sudo Y., Nakaike S., Yamagishi T., *Cancer Chemother. Pharmacol.*, **26**, 83—87 (1990).
4) *a*) Breslauer K. J., Remeta D. P., Chou W.-Y., Ferrante R., Curry J., Zaunczkowski D., Snyder J. G., Marky L. A., *Proc. Natl. Acad. Sci. U.S.A.*, **54**, 8922—8926 (1987); *b*) Pemeta D. P., Mudd C. P., Bergen R. L., Breslauer K.J., Biochemistry, **32**, 5064—5073 (1993).
5) Scaria P. V., Shafer R. H., *J. Biol. Chem.*, **266**, 5417—5423 (1991).
6) *a*) Wilson W. D., Jones R. L., *Adv. Pharmacol. Chemother.*, **18**, 177—222 (1981); *b*) Wilson W. D., Strekowski L., Tanious F. A., Watson R. A., Mokrosz J. L., Strekowska A., Webster G. D., Neidle S., *J. Am. Chem. Soc.*, **110**, 8292—8299 (1988).
7) Inohara T., Tarui M., Mihara Y., Doi M., Ishida T., *Chem. Pharm. Bull.*, **43**, 1607—1613 (1995).
8) Lerman L. S., *J. Mol. Biol.*, **3**, 18—30 (1961).

9) Walker G. T., Stone M. P., Krugh T. R., *Biochemistry*, **24**, 7462—7471 (1985).
10) *a*) Rao K. E., Dasgupta D., Sasisekharan V., *Biochemistry*, **27**, 3018—3024 (1988); *b*) Wells R. D., Larson J. E., Grant R. C., Shortle B. E., Cantor C. R., *J. Mol. Biol.*, **54**, 465—497 (1970).
11) Cantor C. R., Warshaw M. M., Shapiro H., *Biopolymers*, **9**, 1059—1077 (1970).
12) *a*) Rodger A., *Methods Enzymol.*, **226**, 232—258 (1993); *b*) McCoubrey A., Latham H. C., Cook P. R., Rodger A., Lowe G., *FEBS Lett.*, **380**, 73—78 (1996).